Robust Control Strategy to Parameter Variations for an Interior PM Synchronous Machine

VASILE HORGA, DORIN LUCACHE, MARCEL RĂȚOI,
ALECSANDRU SIMION, MIHAI ALBU
Faculty of Electrical Engineering
"Gh. Asachi" Technical University of Iaşi
53 D. Mangeron Blvd., Iaşi, 700050
ROMANIA
horga@tuiasi.ro, lukake@tuiasi.ro, http://www.ee.tuiasi.ro

Abstract: - The interior permanent magnet (IPM) synchronous machines have several desirable features for automotive, tools machines and residential drive applications. When operating over a wide speed range, the main problem is to assure a proper and automatically set flux weakening. The paper presents a control structure of an IPM synchronous machine proper to be used also in the motoring regime, generating regime or in an integrated starter-generator regime. The control algorithm assures insensitivity to the load parameters variation. Experimental results for both cranking and generation are shown and analyzed.

Key-Words: - synchronous machine**,** interior permanent magnet, flux weakening, vector control

1 Introduction

Due to their high efficiency, the permanent-magnet (PM) synchronous machines with constant rotor flux have been attracting wide attentions and extensively used. A special attention was paid to find the existing electric machines that meet the specifications on cranking torque, driving power and speed range at the same time. The continuous cost reduction of magnetic materials with high energy density and coercitivity led to consider the PM synchronous machines as high attractive candidates both in automotive, tools machines and residential drive applications.

One of the exciting automotive application is the integrated starter generator (ISG) that uses one machine to replace conventional starter and alternator onboard vehicles and provides greater electrical generation capacity and improves the fuel economy and emissions. The ISG is coupled to the combustion engine either directly or by a belt.

Nowadays much of the work was done to get the best substitute of the old Lundell alternator. Unlike the machine in pure electric vehicle, the ISG machine has to enable the charging of the battery and to operate electric loads with nearly constant voltage at the speed range corresponding to the engine speed from idle 600rpm to redline 6000rpm.

The IPM motors due to their saliency develop supplementary reluctance torque and thus present a higher torque capability than the surface-mounted permanent magnet synchronous machine (SPMSM). This is why the IPM synchronous machine (IPMSM) is more suited to play the role of an ISG.

The main requirements of the ISG control are to ensure the necessary high torque as starter and the constant output voltage, irrespective of the input speed and load, as generator.

Because of its geometry, IPMSM has a robust rotor construction, a rotor saliency and the low effective air gap. The IPMSM control is done usual by two kinds of methods: direct torque control [1], [2] and vector control [3].

However, as the speed increases, the back electromotive force also increases, so the IPMSM acting as an ISG must operate well in both the constant torque region and the constant power region. To get this, some various control algorithms for flux weakening have been published mainly in the last two decades [4]..[10]. The constant torque region and constant power region are governed by different equations. In time two types of approaches have been used to control the IPMSM: the ancient one is based on the machine equations [7], which can generate problems at the regime switching, and the newest one that apply different control techniques by continuous adjustment of the reactive current at the condition of bounded voltage and current [8], [9]. Our proposed control strategy belongs to the last one and is based on the voltage error.

The IPMSM was controlled in order to be insensitive to the load parameters variation and the control algorithm was tested in different regimes:

motoring, generating and then playing the role of an ISG. The control algorithm is a combination of some techniques found in the literature and is based on the maximum torque-per-ampere strategy (minimum copper loss). A prototype system was tested in order to confirm the control algorithms and dSPACE based experimental results are presented and discussed.

2 Voltage and current limits

In the *d-q* axis synchronous frame, the dynamic equations of the IPMSM can be expressed as:

$$\begin{cases} u_{sd} = R_s i_{sd} + L_d \dfrac{di_{sd}}{dt} - \omega_e L_q i_{sq} \\ u_{sq} = R_s i_{sq} + L_q \dfrac{di_{sq}}{dt} + \omega_e L_d i_{sd} + \omega_e \psi_m \end{cases} \quad (1)$$

Symbols u and i denote voltage and current, ψ_m the flux linkage of the permanent magnets in the *d*-axis rotor, L_d is the *d*-axis self-inductance, L_q is the *q*-axis self-inductance, ω_e is the electrical speed, respectively, and index *s* denotes parameters and variables associated with stator.

The developed electromagnetic torque t_e in terms of stator currents is expressed as:

$$t_e = p\left[\psi_m i_{sq} + \left(L_q - L_d\right) i_{sd} i_{sq}\right] \quad (2)$$

where p denotes the number of pole pairs. This has two components: the alignment torque produced by the flux linkage and the reluctance torque produced by the saliency. It is desirable that the reluctance torque should be properly utilized in order to increase the whole efficiency of the IPMSM drives.

At the low speed, the back-electromotive force is small and so there is enough voltage to control the current to generate the torque. As the rotor speed increases, the marginal voltage to control the current is decreased and the torque becomes highly distorted so the flux weakening method should be applied [4]. The extension range of the speed is solely limited by the structure and the parameters of the motors under the given condition of voltage and current limitation.

The maximum voltage $U_{s\,max}$ that the inverter can supply the machine is limited by DC link voltage and PWM strategy. When the voltage space vector strategy is used, $U_{s\,max} = U_{DC}/\sqrt{3}$. Also the maximum current $I_{s\,max}$ is determined by the inverter current rating and machine thermal rating.

So, the imposed limits for the motor's voltage and current are:

$$\begin{cases} u_{sd}^2 + u_{sq}^2 \le U_{s\,max}^2 \\ i_{sd}^2 + i_{sq}^2 \le I_{s\,max}^2 \end{cases} \quad (3)$$

Neglecting the stator resistance (when speed increases the term ω_e becomes more important), from (1) the steady-state voltage limit equation yields:

$$\left(i_{sd} + \frac{\psi_m}{L_d}\right)^2 \left(\frac{L_d}{L_q}\right)^2 + \left(i_{sq}\right)^2 \le \left(\frac{U_{s\,max}}{\omega_e L_q}\right)^2 \quad (4)$$

From (3) and (4) it can be seen that the current limit equation determines a circle with a radius of $I_{s\,max}$, while the voltage limit equation determines a series of nested ellipses (for the IPMSM, $L_q > L_d$). Fig.1 shows the current-limit circle and the voltage-limit ellipses in the i_{sd}-i_{sq} plane.

The voltage-limit ellipse decreases as the speed increases. At a so-called base speed ω_{base}, the maximum torque point *A* is on the cross point of maximum torque-per-current trajectory and current-limit circle. When the IPMSM is operated from the start up to the base speed in the constant torque region, the voltage-limit ellipse exceeds the maximum current boundary and no voltage limitation needs to be considered in this situation.

But beyond the base speed, the IPMSM cannot be operated without flux-weakening control and so, to extend the speed range, a proper demagnetizing current has to be applied depending on the operating speed. The current vector trajectory will move along the boundary of the current-limit circle (from A to B in Fig.1) as rotor speed increases.

Without a proper flux weakening at higher speed, the current regulators would be saturated and lose their controllability. Since the onset of current regulator saturation varies according to the load conditions and the machine parameters, the beginning point of the flux weakening should be varied. The late starting of the flux weakening may result in undesired torque drop, but the early starting deteriorates the acceleration performance [5].

3 The control algorithm

As opposed to SPMSM, the i_d=0 control method is not suitable for the IPMSM because the reluctance torque is not produced even if this kind of machine has a saliency.

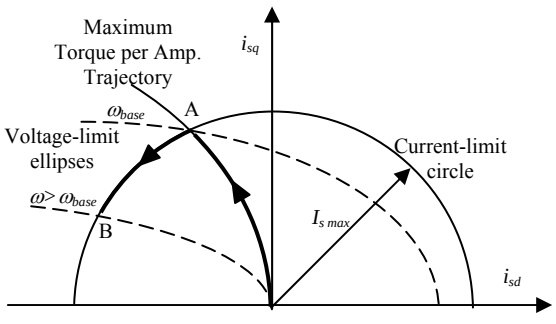

Fig.1 Current-limit circle and voltage-limit ellipses in the i_{sd}-i_{sq} plane

At low speeds, because the absence of voltage limitation, the current vector might be controlled to fully use reluctance torque in order to maximize the machine efficiency. Typically, it is chosen to maximize the torque per amper ratio by controlling the current vector in order to have an optimum inclination versus *q*-axis. To get the maximum torque control, the inclination angle γ of the current vector (Fig.2) depends on the load conditions, taking values between 0 and 45° [6].

The maximum torque-per-ampere (MTPA) strategy seeks to get a certain torque with the smallest possible stator current amplitude (so with minimum copper loss). Because $i_{sd} = -i_s \sin\gamma$ and $i_{sq} = i_s \cos\gamma$, where $i_s = |\underline{i_s}|$, (2) becomes:

$$t_e = p\left[\psi_m i_s \cos\gamma + \frac{1}{2}\left(L_q - L_d\right) i_s^2 \sin 2\gamma\right] \quad (5)$$

and imposing the condition :

$$dt_e / d\gamma = 0 \quad (6)$$

the relation between i_{sd} and i_{sq} for the maxim torque per amper control is derived as

$$i_{sd} = \frac{\psi_m}{2\left(L_q - L_d\right)} - \sqrt{\frac{\psi_m^2}{4\left(L_q - L_d\right)^2} + i_{sq}^2} \quad (7)$$

This relation is shown as the maximum torque-per-ampere trajectory in Fig.1.

Above the base speed, the normal operation is possible only applying the flux weakening and the maximum torque is obtained when the drive operates in the voltage and current limits. The flux weakening control of IPM synchronous machines is conducted by injecting the *d*-axis current i_{sd} negatively, which is different from induction machine where the flux is weakened by decreasing the *d*-axis current.

However, another relation between i_{sd} and i_{sq} could be established and so the control in the constant torque region and constant power region is based on different equations. Some authors, as [6], proposed an algorithm for the control mode transition, but all kind of transitions can lead to instability. The authors of [4] proposed another method by adjusting the *d*-axis current command depending as well as the bounds of the maximum *q*-axis current of the speed controller in the following manner: the *d*-axis current is fixed as a transient which is initiated such that the *q*-axis current bound can be gradually adjusted by a PI controller. The corresponding *q*-axis bound is calculated simultaneously as the PI controller adjusts the *d*-axis current, but it is found that under transient conditions cannot follow the true bounds instantaneously. A field weakening control scheme based on a real-time adjustment is present also in [7], but the used

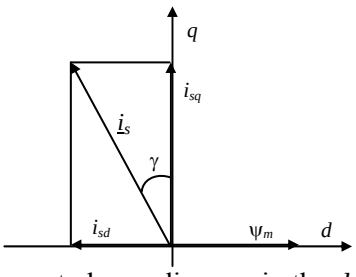

Fig.2 Current phasor diagram in the *d*-*q* frame

maximum torque-per-ampere strategy lead to inadequate torque at high speeds and light loads. In [8] the flux weakening control algorithm takes into account the error between the maximum voltage and the command voltage and the flux weakening could be set to prevent the saturation of the current regulators. Other authors like [9] pointed out that the PI controller should be replaced by an integral (I) controller, to either ensure the drive stability or simplify the controller design. In order to eliminate the gradual adjustment by feedback mechanisms so as to achieve faster response and better stability, [10] proposed o new flux-weakening control method based on a closed-form solution of the available maximum torque.

The proposed control strategy is an improved combination of the previous discussed techniques based on the voltage error. The Fig.3 presents the schemes used in the three operating cases: motoring, generating and ISG, the block components being detailed in the last one.

The *d*–axis and *q*-axis currents cannot be controlled independently by u_{sd} and u_{sq} because of the cross-coupling effects (the terms $\omega_e L_q i_{sq}$ and $\omega_e L_d i_{sd}$ in (1)) that are dominant for IPMSM due to relatively large inductances and increase as the speed increases. The cross-coupling effects are usually canceled by the feedforward compensation [6].

Two PI controllers, implemented in the synchronous reference frame, are used for the current control, followed by a decoupling circuit. In the constant power operation, a closed-loop voltage control is used to ensure an automatically onset of the accurate flux-weakening operation, depending on the load condition and machine parameters. Flux weakening mode is entered when the error

$$\varepsilon = u_{s\,max}^2 - \left(u_{sd}^2 + u_{sq}^2\right) \quad (8)$$

becomes negative. This error, passing through a low-pass filter (LPF) and regulated by an I controller, lead to the *d*-axis current increases toward the negative direction to prevent saturation of the current regulators. The I controller output is limited (to avoid irreversible demagnetization) so that the *d*-axis current to be between 0 and the minimal allowable

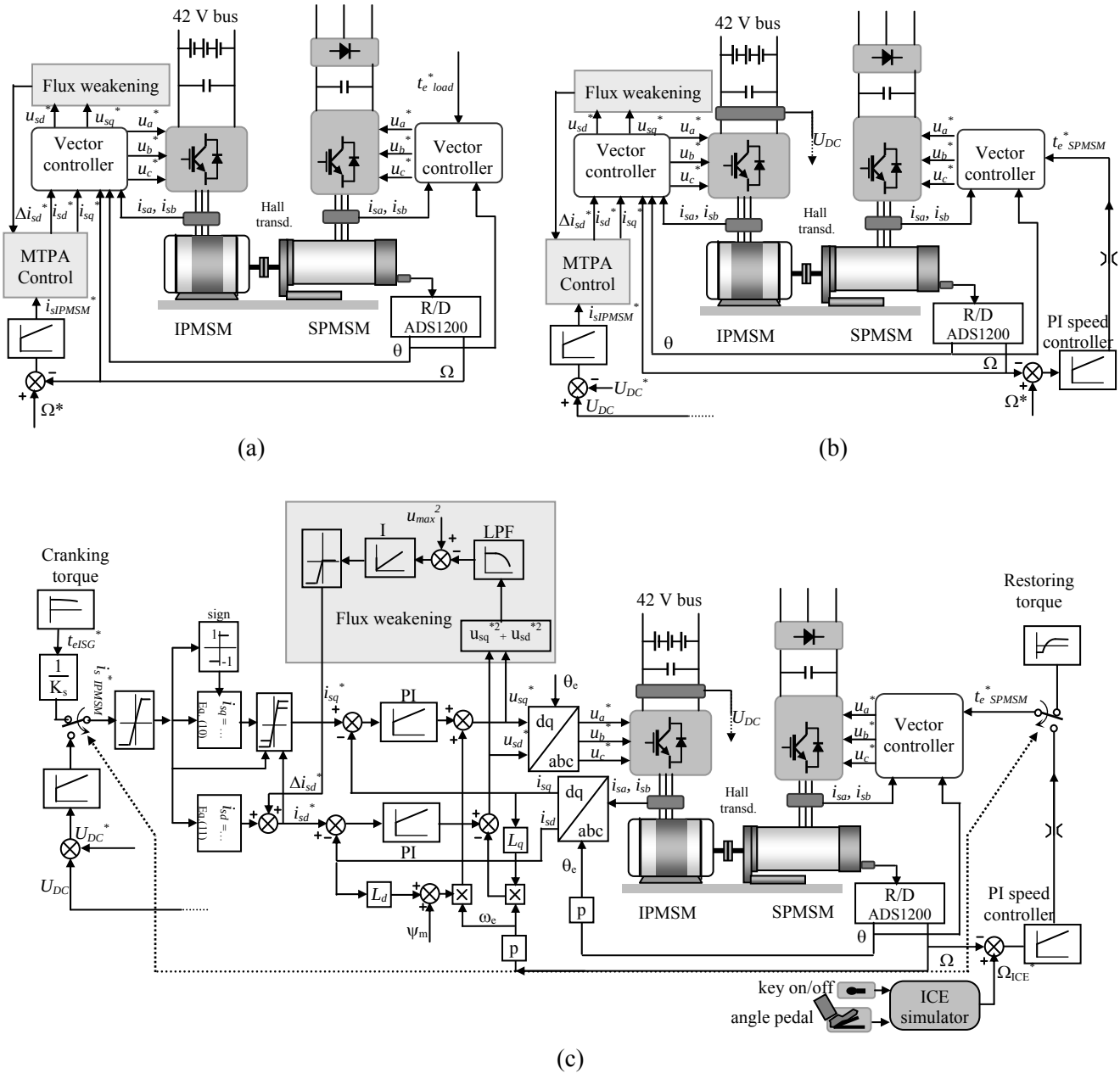

Fig.3 The control schemes: (a) – motoring regime, (b) – generating regime, (c) – ISG regime

$i_{sd}^* = -I_{sd\,max}$.

The magnitude of the injected stator current i_s can be expressed as

$$i_s = \sqrt{i_{sd}^2 + i_{sq}^2} \tag{9}$$

and taking into account (7), the *d*-*q* axis components of the current vector that ensures the maximum torque-per-ampere yields

$$i_{sq} = sign(i_s) \cdot \sqrt{i_s^2 - i_{sd}^2} \tag{10}$$

where

$$i_{sd} = \frac{\psi_m - \sqrt{\psi_m^2 + 8(L_q - L_d)^2 i_s^2}}{4(L_q - L_d)} \tag{11}$$

The last equation is equivalent with (7) but expressing the *d*-axis current as a function of i_s, taking into account (9).

Thus, when the *d*-axis current is increased with respect to the voltage limit, the *q*-axis current is depressed in order to ensure the current limit condition. Moreover, a saturation block with adaptive limits take into account the flux weakening command Δi_{sd}^* and forces once more the operating point to not exceed the current-limit circle. In this way the current regulators regain the ability of regulating the *d*-axis and *q*-axis currents and the maximum torque-per-ampere is produced at the crossing point between the current limit circle and voltage limit ellipse, in the constant power region.

Because this scheme utilizes for flux weakening the output voltage of the PI current regulators and the outer voltage-regulating loop instead of the IPMSM model, it becomes robust and insensitive to load conditions and load parameters.

The external lead-acid battery pack has a double role: provides the energy necessary in the ISG motoring mode and stores the energy produced in the generating mode. A capacitive filter is connected to the DC line.

4 Experimental results

In this paper a commercial IPMSM, designed for playing as automotive generator, operating at low voltage and high currents, was used (rated parameters in Table 1). This is mechanical coupled (Fig.4) to an internal combustion engine simulator that consists in a SPMSM (1.9 kW, 330V, 4.4A and 4000rpm). The speed of the engine simulator can be varied in closed loop by means of its own inverter.

The engine simulator is based on a mean torque predictive engine model, which would take into account the major dynamics (lag and delays) inherent in the spark ignition torque production process [12]. Though the obtained speed characteristics may be different from a real engine, and the power ratio between ISG and engine simulator is not proper, this experimental setup allows testing the validity of the proposed control algorithms successfully.

Table1 IPM synchronous machine characteristics

Rated power [kW]	4
Peak current constraint [A]	160
Number of phases	3
Number of poles	12
R_s [mΩ]	21
L_d [mH]	0.076
L_q [mH]	0.12
ψ_m [Wb]	0.009
Rated speed [rpm]	2000
Rated voltage [V]	11

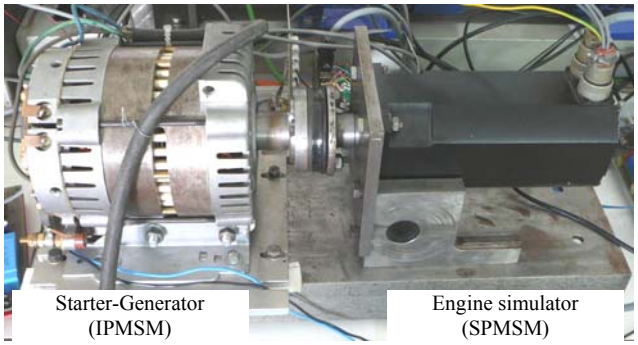

Fig.4 View of the test bench

The PWM converter connected to IPMSM is a standard three-phase bridge that is capable of bi-directional power flow. In the ISG motoring mode this converter acts as an inverter and in the generating mode it acts as a boosting rectifier. A few years ago, the automobile industry agreed to adopt standards for a new 42V voltage for production and use of electrical power. This new standard was not adopted in a rush and various system voltage ranging from 42V to 500V were proposed.

To control the whole experimental system, a dSPACE 1104 board and ControlDesk software is being used. This board contains all the peripherals and resources necessary to control simultaneously both the load machine (engine simulator) and IPMSM. The speed information comes from the resolver included in the SPMSM and is digitalized with an ADS1200 resolver-to-digital converter. For the currents and the voltages measure the Hall transducers are used.

4.1 IPMSM motoring regime

The control scheme corresponds to Fig.3.a and the IPMSM base speed was estimated of about 1200rpm. The Fig.6 catch the moments when the IPMSM starts-up in the motoring regime for a time

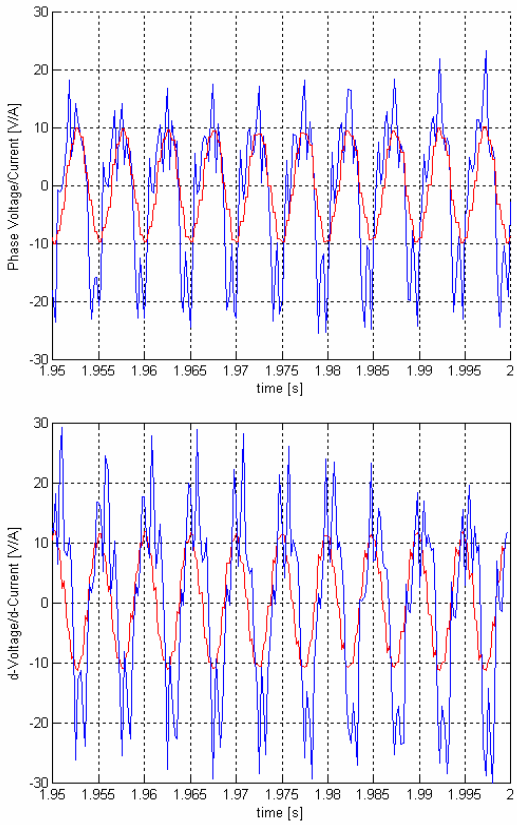

Fig.5 The phase- and *d*-axis voltage and currents

interval of two seconds, both bellow and above the base speed. The high DC current/phase current demand can be noticed up the system stabilizes at the reference speed.

Due to its specific geometry and construction, IPMSM produces non-sinusoidal currents, as seen in Fig.5. These currents are acquired and used to generate the reference voltage commands. The reference and measured currents in the d-q frame are presented in Fig.8. The current and voltage space phasor loci in the stationary reference frame presented in Fig.7 confirm the presence of the fifth harmonic in the phase current of the IPMSM [13]. More, Fig.8 shows how the flux-weakening block acts with Δi_{sd}^{*} to prevent the regulators saturation when the base speed is surpassed.

4.2 IPMSM generating regime

In the generating regime, the PWM inverter boosts up to about 38V on the DC link, charging the batteries pack with a low current (approx. 1.2A) as seen in Fig.9.b While the battery pack is connected, this will keep the DC voltage approximately constant during non-high load variations.

As in the previous case, the current and voltage space phasor loci in the stationary rotating reference frame presented in Fig.10 confirm the presence of the fifth harmonic in the phase current of the IPMSM, issue that causes many oscillations of the

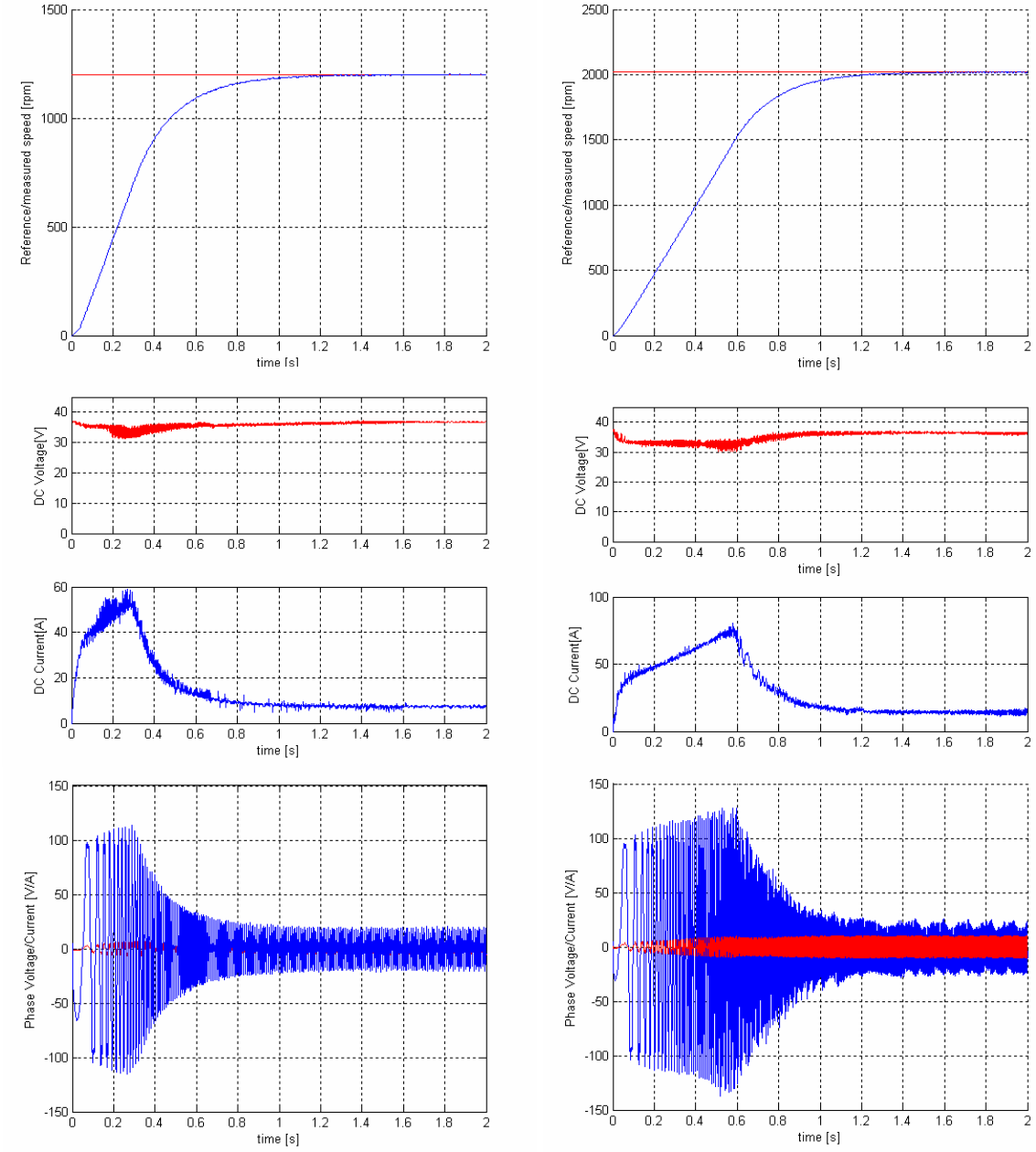

Fig.6 Experimental results bellow (left side) and above (right side) the base speed

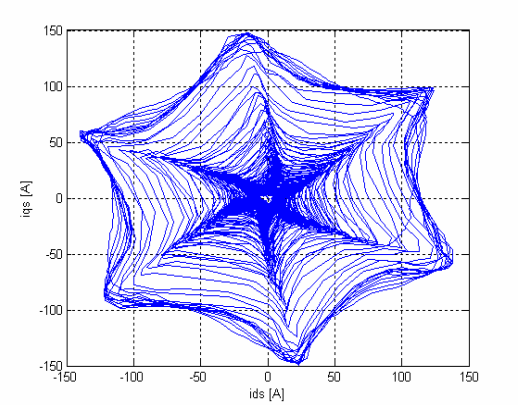

Fig.7 Current space phasor loci in the stationary reference frame bellow the base speed

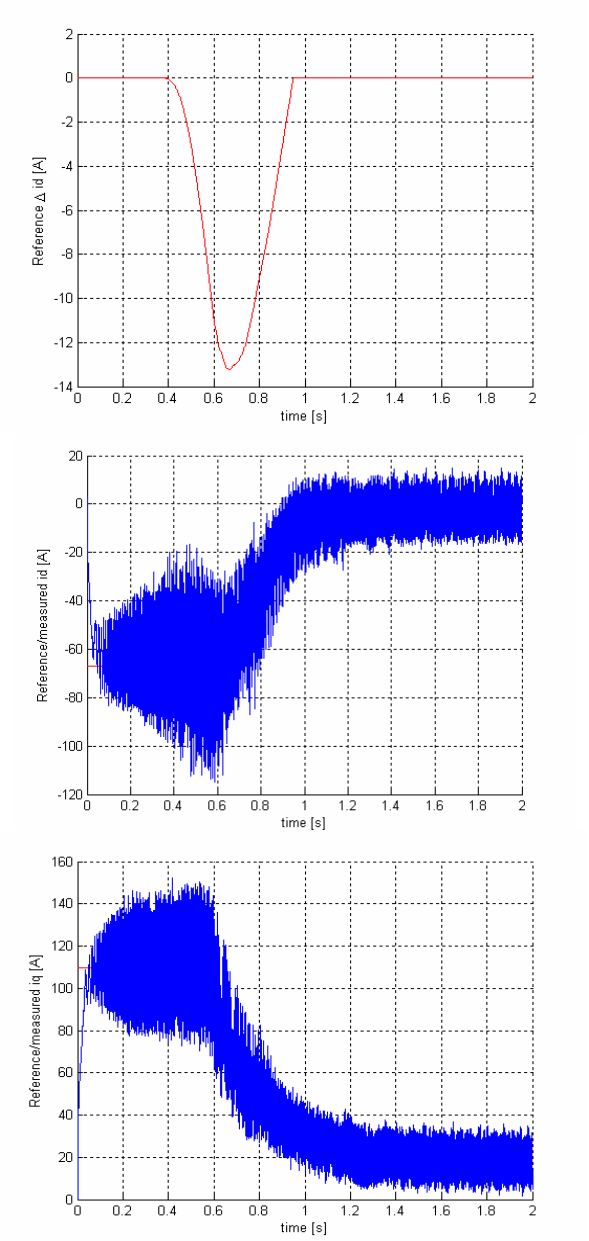

Fig.8 Reference and measured currents in the *d-q* frame

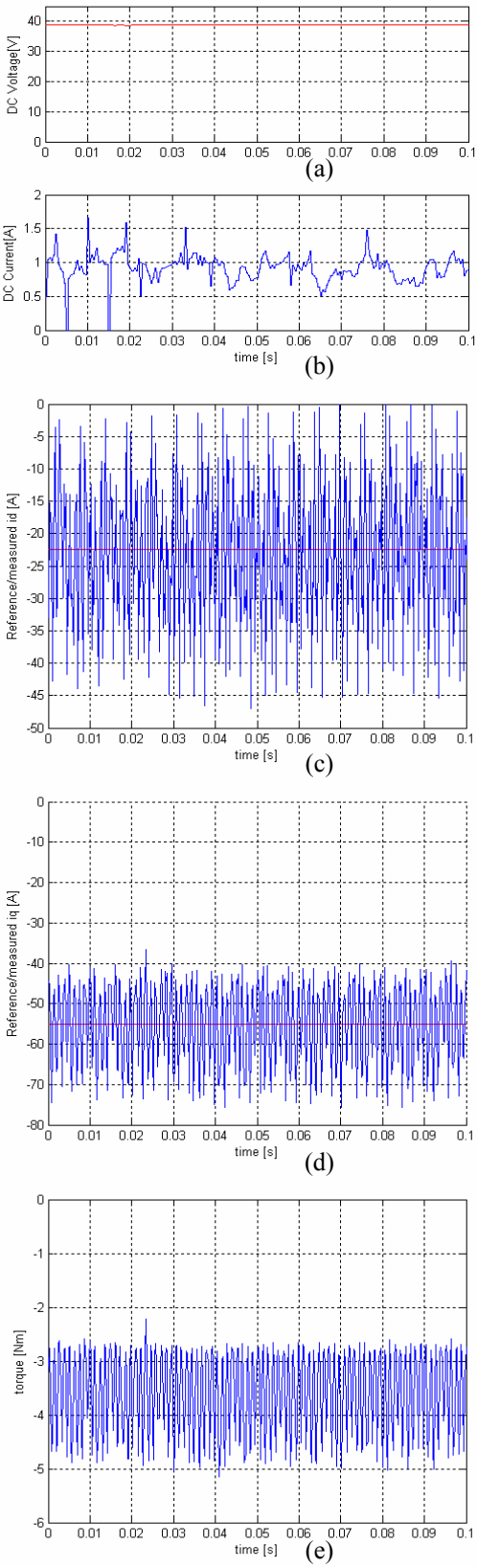

Fig.9 Experimental obtained values for the IPMSM in generating regime

generated i_d and i_q currents as we can see in Fig.9.c and Fig.9.d. In the absence of the corresponding transducer, Fig.9.e shows the estimated electromagnetic torque.

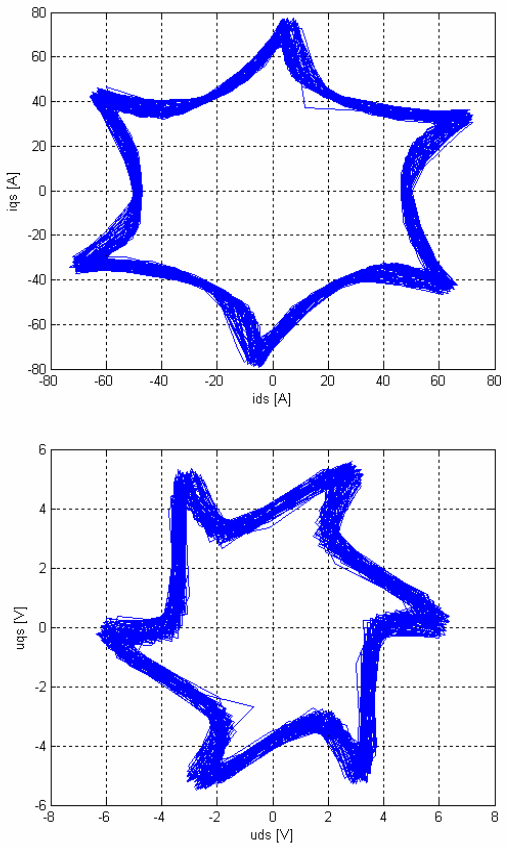

Fig.10 Current and voltage space phasor loci in the stationary reference frame

4.3 IPMSM as integrated starter-generator

The conceived control algorithm was tested as part of an integrated-starter-generator system. The considered time interval was set again at two seconds. In the first moments, during 0.28 sec, the engine is cranked by the ISG from 0 up to 600 rpm. As motor, the ISG takes a large current from batteries to generate the necessary cranking torque. Once the speed gets 600 rpm, the engine control system switches on the speed loop, producing acceleration up to the reference cruise speed (in our case 1200 rpm).

At the same time, the ISG control system changes from the motoring to generating regime. In the generating regime, the PWM inverter boosts up to about 38V on the DC link, charging the batteries pack as previously (Fig.11).

Once the start-up period was surpassed, the system will keep the engine-imposed speed and the same output voltage, the DC voltage being approximately constant because the connected batteries pack.

The experimental results presented in Fig.12 and 13 are, as expected, a mixture of the previously studied regimes and show good system stability to the regime switching from motoring to generating.

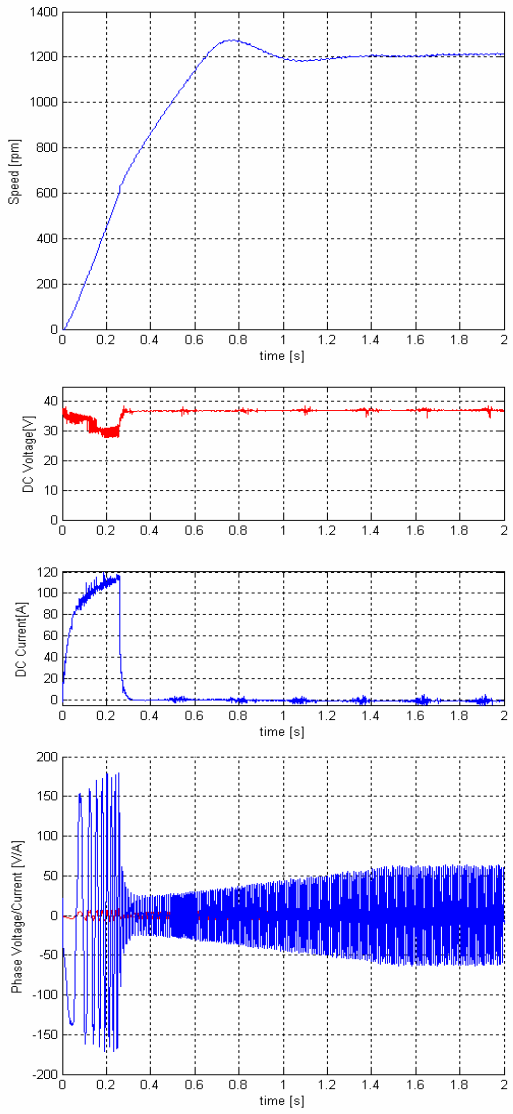

Fig.11 External characteristics of the ISG system

5 Conclusions

This paper has provided a control solution for an IPMSM using the vector control technique in order to get high performances as requested in automotive applications. The proposed system is implemented both as a torque control scheme in motoring mode and as output voltage control scheme in generating regime when the IPMSM is driven by an engine simulator.

A laboratory prototype for the ISG system has been implemented to validate the proposed method. The results of the paper suggest that the controlled IPMSM responds to the specific demands in different operating conditions and offers good dynamic performances.

Two difficulties we have had to surpass in the testing experiments. First, the low design characteristics of the IPMSM that produces a high

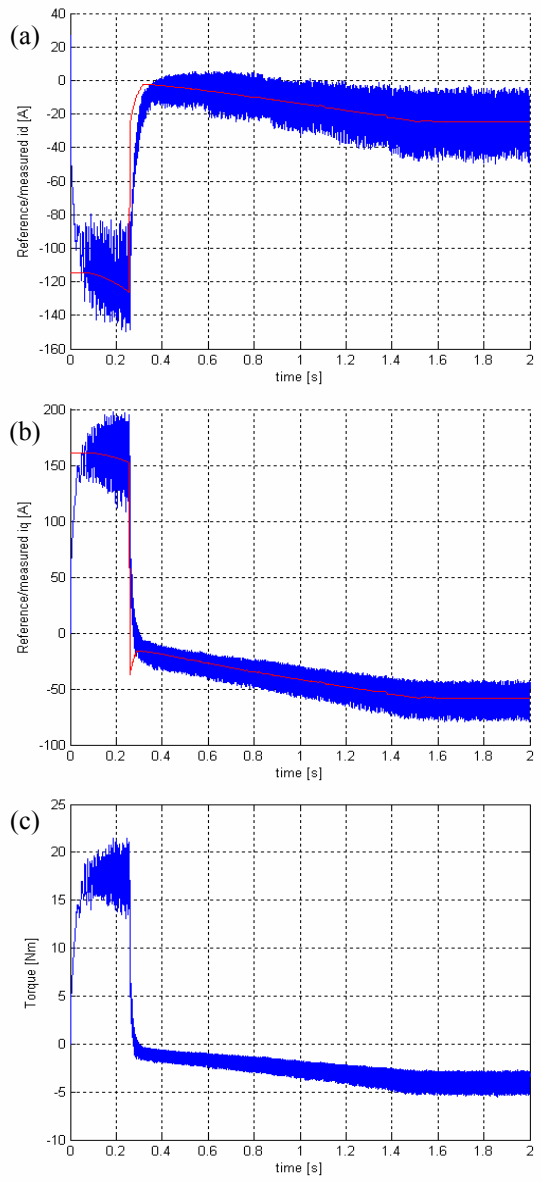

Fig.12 The reference and measured i_d , i_q currents and the estimated electromagnetic torque t_e

fifth-harmonic in its phase currents and so hardly influences the generated reference command-voltages. Second, the PWM converter connected to IPMSM is built with IGBT devices. These ones have a high voltage drop and become difficult to use the converter at low voltages, as requested in many specific automotive applications.

In a future research we intend to apply the conceived control algorithm to a hybrid-excited synchronous machine, taking into account the minimum loss criterion as in [11].

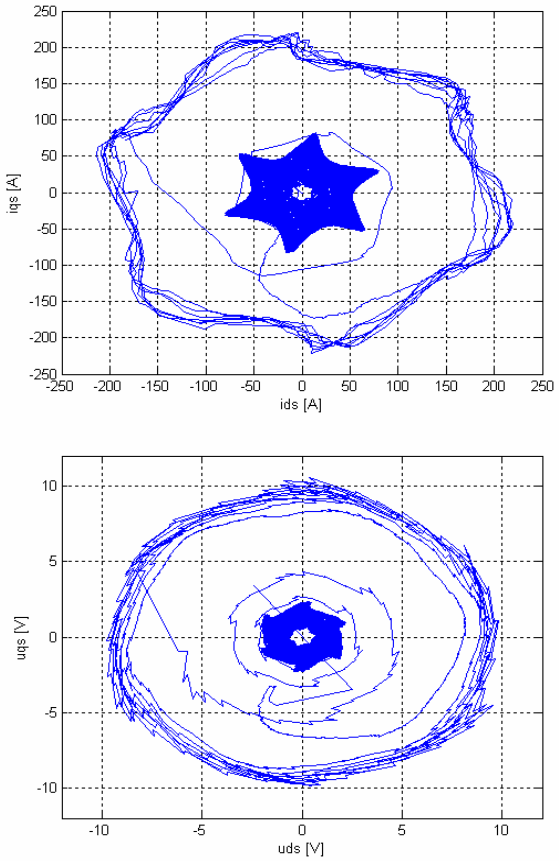

Fig.13 Current and voltage space phasor loci in the stationary reference frame

References:

[1] G. Noriega, M. Strefezza, Direct torque control of a permanent magnet synchronous motor using fuzzy logic**,** *Proc. of the 7th WSEAS International Conference on Power Systems*, Beijing, China, September 15-17, 2007

[2] S.V. Paturca, M. Covrig, L. Melcescu, A modified direct torque control scheme for permanent magnet synchronous motor drives, *WSEAS Transactions on Systems and Control*, Issue 2, Volume 1, December 2006, ISSN 1991-8763, pp.135-140

[3] P.Vas, *Vector Control of the AC Machines*, U.K.Oxford University Press, 1990

[4] J. H. Song, J. M. Kim, and S. K. Sul, A new robust SPMSM control to parameter variations in flux weakening region, *IEEE IECON*, vol. 2, pp. 1193-1198, 1996.

[5] Y. S. Kim, Y. K. Choi and J. H. Lee, Speed-sensorless vector control for permanent-magnet synchronous motors based on instantaneous reactive power in the wide-speed region, *IEE Proc-Electr. Power Appl.*, vol. 152, No. 5, pp. 1343-1349, Sept. 2005.

[6] S. Morimoto, M. Sanada and K. Takeda, Wide-speed operation of interior permanent magnet synchronous motors with high performance current regulator, *IEEE Trans. Ind. Applicat.*, vol. 30, pp. 920-926, July/Aug. 1994.

[7] J.Wai, T.Jahns, A new technique for achieving

wide constant power speed operation with an interior PM alternator machine, *Proc. of IEEE Ind. Appl. Society Annual Meeting*, Chicago, IL, Oct. 2001

[8] J. M. Kim and S. K. Sul, Speed control of interior permanent magnet synchronous motor drive for the flux weakening operation, *IEEE Trans. Ind. Applicat.*, vol. 33, pp. 43-48, Jan./Feb. 1997.

[9] N.Bianchi, S.Bolognani, High-performance PM synchronous motor drive for an electrical scooter, *IEEE Trans. on Industry Applications*, vol.37, no.5, Sept./Oct.2001, pp.1348-1355

[10] C-T. Pan, S-M. Sue, A linear maximum per ampere control for IPMSM drives over full-speed range, *IEEE Trans. on Energy Conv.,*Vol.20, No.2, June 2005, pp.359-366

[11] S.Shinnaka, T. Sagawa, New optimal control current methods for energy efficient and wide speed-range operation of hybrid-field synchronous motor, *IEEE Int. Conf. on Electric Machines and Drives*, May 2005, pp. 535 – 542

[12] D.Lucache, V.Horga, M.Ratoi, M.Albu, Hardware-in-the-loop testing of an integrated starter alternator, *Proc. Of Joint Conferences ACEMP'07 & Electromotion'07*, September 2007, Bodrum, Turkey, pp.363-368

[13] P. Vas, *Parameter Estimation, Condition Monitoring, and Diagnosis of Electrical Machines*, Clarendon Press, Oxford, 1993

[14] A. Nait Seghir, M.S. Boucherit, Artificial Neural Network to Improve Speed Control of Permanent Magnet Synchronous Motor**,** *Proc. of the 6th WSEAS/IASME Int. Conf. on Electric Power Systems, High Voltages, Electric Machines*, Tenerife, Spain, December 16-18, 2006

[15] M. Rashidi, A Robust and Adaptive RBF Neural Network Based on Sliding Mode Controller for Interior Permanent Magnet Synchronous Motors, *Proc. of the 5th WSEAS/IASME Int. Conf. on Electric Power Systems, High Voltages, Electric Machines*, Tenerife, Spain, December 16-18, 2005, pp.46-51